PHYSICAL REVIEW A VOLUME 57, NUMBER 6 JUNE 1998

Bose-Einstein condensation of large numbers of atoms in a magnetic time-averaged orbiting potential trap

D. J. Han, R. H. Wynar, Ph. Courteille, and D. J. Heinzen
Department of Physics, The University of Texas, Austin, Texas 78712
(Received 23 January 1998)

We have observed Bose-Einstein condensation of large numbers of ^{87}Rb atoms in a magnetic time-averaged orbiting potential (TOP) trap. Over 1.5×10^9 atoms are captured in the trap and evaporatively cooled to produce condensates containing up to 2×10^5 atoms. We discuss special considerations relating to the production of large Bose-Einstein condensates in a TOP trap, and present measurements of the condensate fraction for this case. [S1050-2947(98)50806-2]

PACS number(s): 03.75.Fi, 05.30.Jp, 32.80.Pj

Bose-Einstein condensation (BEC) of a dilute atomic gas has recently been achieved in rubidium [1–4], lithium [5], and sodium [6–8]. This development provides us with an unprecedented opportunity to study nearly ideal Bose-condensed gases. One of the most exciting possibilities is that processes related to BEC will allow us to produce a coherent matter wave source, or ''atom laser'' [9]. In order to realize BEC, atoms are first laser-cooled, then transferred into a magnetic trap, and then further cooled by evaporation [10]. During evaporative cooling, the hottest atoms are selectively ejected from the trap, and the remaining atoms rethermalize at successively lower temperatures due to elastic collisions. This method requires strong magnetic forces in order to achieve sufficient atomic density and collision rate. A spherical quadrupole magnetic field provides the tightest confinement for a given magnetic coil current and size. However, this configuration cannot produce a BEC because atoms are lost from the trap due to Majorana spin-flip transitions at the field zero in the trap center [11,12]. Three field configurations have been successful: a quadrupole magnetic trap in which atoms are prevented from reaching the field zero by the optical dipole force of a focused laser beam [6], the Ioffe-Pritchard trap, which lacks the field zero [2,3,5,7,8], and the time-averaged orbiting potential (TOP) trap [1,4]. The TOP trap was the first to successfully produce BEC [1]; it has the advantage that it can provide relatively strong confinement with modest trap asymmetry at the same time. However, previous experiments with this trap have produced only relatively small condensates containing at most about 5000 atoms [13,14]. In this Rapid Communication, we report the production of a BEC of ^{87}Rb atoms in a TOP trap containing up to 2×10^5 atoms, about 40 times as many atoms as has been reported previously [13,14]. This result extends the usefulness of the TOP trap as a source of Bose-condensed atoms [15]. We also report measurements of the condensate fraction for our experimental conditions, and find good agreement with ideal-gas theory.

The TOP trap consists of the superposition of a spherical quadrupole field $B_q'(r\hat{\mathbf{r}}-2z\hat{\mathbf{z}})$ and a rotating bias field of constant magnitude B_b [11]. It displaces the field zero into a circular orbit of radius $r_d=B_b/B_q'$. For a sufficiently fast rotation, the atoms respond only to the time-averaged potential. This potential is axially symmetric and harmonic for small displacements, with trap frequencies $\omega_r=(\mu B_q'^2/2mB_b)^{1/2}$ and $\omega_z=\sqrt{8}\omega_r$, where m is the mass of the atom and μ its magnetic moment. If r_d is sufficiently large, the Majorana losses are suppressed because the orbiting field zero lies well outside the atomic cloud.

Majorana losses at the orbiting field zero can make it somewhat difficult to produce a large condensate in a TOP trap. In order to initiate evaporative cooling, the elastic collision rate of the atoms must be large. This is usually achieved in part with an adiabatic compression of the atomic density by the magnetic trapping potential. In order to compress the cloud in a TOP trap, we must increase B_q' or decrease B_b. Unfortunately, this also decreases $r_d/r_0 \sim B_b^{3/4}/B_q'^{1/2}$, where r_0 is the rms radius of the trapped atom cloud. A large cloud will tend to have a modest initial value of r_d/r_0, since the maximum value of r_d is constrained by the available field strengths and by the need to produce a field curvature sufficient to capture the cloud of atoms. In

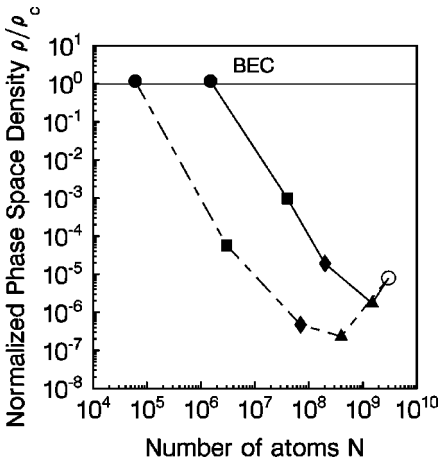

FIG. 1. Phase-space density, in units of the phase-space density at the BEC transition point, vs atom number at different stages after the TOP trap loading. Solid line, initial $B_b=30$ G; dashed line, initial $B_b=20$ G. The stages indicated are dark molasses cooling (open circle), optimized TOP trap loading (triangles), compression and evaporation by increasing B_q' (diamonds), evaporation and compression by decreasing B_b (squares), and rf-induced evaporation (filled circles). (For the optical molasses point, we neglect the lack of atomic spin polarization in calculating phase-space density.)

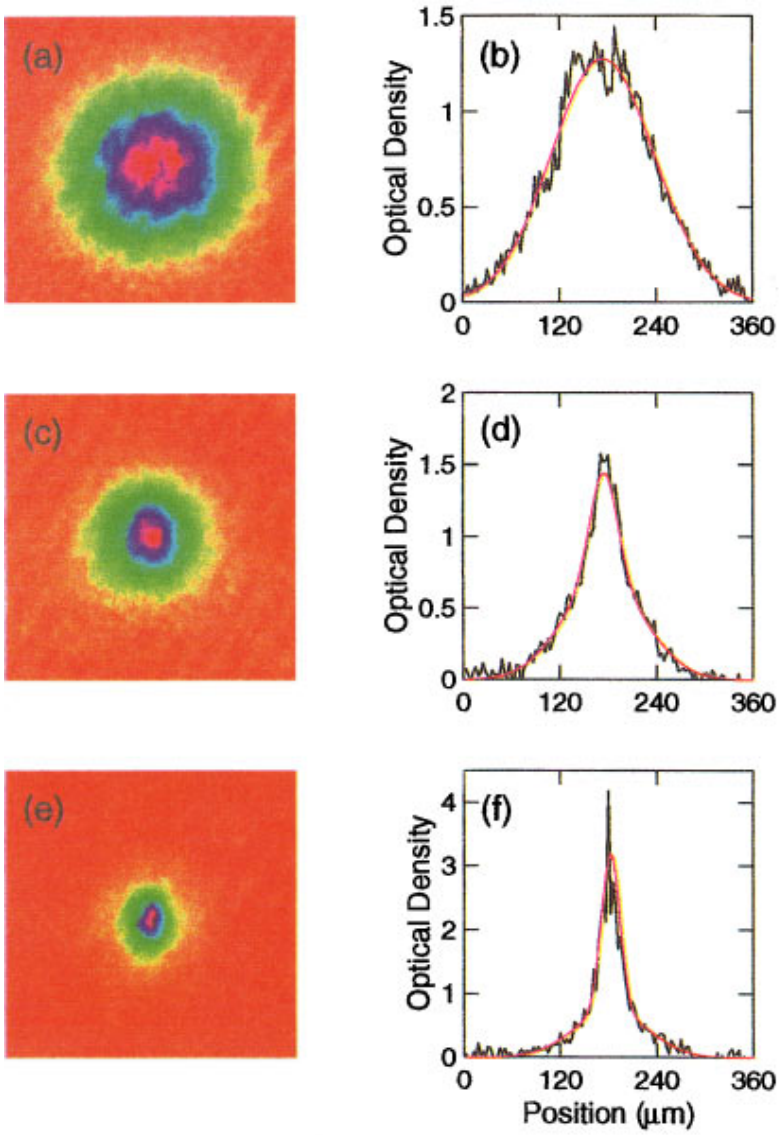

FIG. 2. (color) (a),(c),(e) 360 μm$\times$360 μm false-color absorption images of evaporatively cooled clouds released from the TOP trap after a free expansion time of 18 ms. (a) Temperature just above T_c; (c) temperature just below T_c; (e) temperature further below T_c. The vertical direction is aligned with the symmetry axis of the TOP trap. (b), (d), (f) One-dimensional cuts through the center of the clouds, showing optical density vs horizontal displacement, for the images (a), (c), and (e), respectively. Below T_c the clouds show a double-peaked structure corresponding to a broad, symmetric thermal distribution, and a narrow, asymmetric condensate peak.

this case, as the TOP trap is compressed the orbiting field zero may cut into the cloud and produce Majorana losses before significant compression has occurred. Therefore, in order to produce a large BEC in a TOP trap, the density must be high enough to evaporatively cool without substantial compression, or the trapping fields must be very large. We have succeeded with the former approach, evaporatively cooling a cloud of $>10^9$ atoms in a TOP trap with $B_q' \leqslant 200$ G/cm, and $B_b \leqslant 30$ G. Substantial magnetic compression of the cloud without Majorana losses would be possible only with much larger fields than this.

We load the TOP trap as follows. We produce a slow atomic ^{87}Rb beam with a velocity of 30 m/s using an increasing field (σ^-) Zeeman slower [16]. Atoms from the slow beam are captured by a bright magneto-optical trap (MOT) [17] formed by six 3.5-cm-diam laser beams with an intensity of 6 mW/cm^2 and detuning of -15 MHz, and an axial magnetic field gradient of 15 G/cm. After loading the MOT for 15 s, we switch to a forced dark MOT for 300 ms in order to compress the atoms. This trap has a 1-cm-diam dark spot in the MOT repumping beams [18], and a 2-mm-diam, 2-mW/cm^2 intensity ''depopulator'' laser beam tuned to force the atoms into the lower ($F=1$) ^{87}Rb hyperfine state [19]. At this stage, we typically trap 5×10^9 atoms at a density of 5×10^{11} cm^{-3}. We then lower the temperature to 40 μK with 5 ms of dark molasses cooling, obtained by detuning the trapping lasers to -50 MHz, lowering their intensity to 3 mW/cm^2, turning off the depopulator, leaving the repumpers with dark spots on, and turning the gradient magnetic field off. We find that this large detuning is essential for good cooling. Following this, we optically pump the atoms into the upper ($F=2$) hyperfine state. Finally, we turn off all the laser beams and suddenly switch the TOP trap on with $B_q'=65$ G/cm, $B_b=30$ G, and a bias field rotation frequency of 7.65 kHz. At this stage, we trap 1.5×10^9 atoms with a temperature of 70 μK and a peak density of 1.5×10^{11} cm^{-3}. The rms cloud radius $r_0=0.173$ cm, whereas $r_d=0.46$ cm and $r_d/r_0=2.7$. The lifetime of the magnetically trapped atoms is 170 s.

Following the loading of the TOP trap, we compress the atomic cloud by first adiabatically ramping B_q' up to 200 G/cm in 8 s, and then ramping B_b down to 8 G in 14 s. Due to the small initial value of r_d/r_0, we do not obtain a large

adiabatic compression without Majorana losses. However, in our case the initial trap-averaged elastic collision rate is about 8 s^{-1}, where the elastic cross section $\sigma = 8\pi a^2$, with $a = 109a_0$ [20]. Because of this, the Majorana losses simply result in evaporative cooling, since they occur at the outer edge of the cloud where the energy per atom is large, and since the elastic collision rate is large enough to rethermalize the cloud as the compression proceeds. After the compression we typically have 4×10^7 atoms at a temperature 15 μK, and peak density 8×10^{12} cm^{-3}, with calculated trap frequencies $(\omega_r, \omega_z) = 2\pi\times$(64 Hz, 181 Hz). We then further cool the atoms with rf-induced evaporation [10–12], ramping the frequency from 10.2 MHz to a final frequency ν_{final} in 25 s. The final frequency determines the final temperature of the atoms.

The phase-space densities obtained in these experiments are shown in the solid line of Fig. 1, as a function of the number of atoms in the trap. We determine the number, density, and temperature of the atoms with a combination of laser-induced fluorescence and absorption time-of-flight imaging. We find that once the evaporative cooling has been initiated, we gain approximately 2.2 orders of magnitude in phase-space density for each order-of-magnitude loss in atom number. This allows us to reach the BEC transition point with 1.5×10^6 trapped atoms. The efficiency is about the same for the Majorana loss-induced evaporation as for the rf-induced evaporation. This efficiency is slightly lower than that obtained in Ioffe-Pritchard traps [7,2]; this may be due to the fact that the evaporation in the TOP trap is of lower dimension than in a Ioffe-Pritchard trap [10]. We also tried rf-induced evaporation simultaneously with the Majorana-induced evaporation, and found that the efficiency was unchanged. In our first experiments, we also tried to obtain efficient evaporation with a maximum value of $B_b = 20$ G. Our best results for this case are shown in the dashed line of Fig. 1. With $B_b = 20$ G, we were not able to avoid a substantial loss of atoms during the initial stages of the trap loading and compression, although we did obtain efficient evaporative cooling during the latter stages.

In order to study the atomic cloud near the BEC transition point, we use time-of-flight absorption imaging. At the end of the rf ramp, we adiabatically reduce the quadrupole field gradient by a factor of 5 in 2 s, so that the final trapping frequencies are $(\omega_r, \omega_z) = 2\pi\times$(11.7 Hz, 33.1 Hz) as determined by a direct measurement of trap oscillations. Finally, we suddenly switch the trap off, and the cold-atom cloud expands for a time τ. We image the expanded cloud by illuminating it with a pulsed laser beam with a 50-μs duration, +9.5-MHz detuning, and 0.4 mW/cm^2 intensity. The shadow cast by the cloud onto the laser beam is imaged onto a charge-coupled-device camera. We convert these absorption images into a two-dimensional plot of the optical density of the expanded cloud. Typical false-color plots for $\tau = 18$ ms are shown in Figs. 2(a), 2(c), and 2(e), for $\nu_{final} = 6.55$, 6.30, and 6.25 MHz, respectively. Above the BEC transition point, the images essentially show the velocity distribution of the clouds. The corresponding optical density along a line through the cloud center and perpendicular to the trap symmetry axis is shown in Figs. 2(b), 2(d), and 2(f).

The BEC phase transition is observed when ν_{final} is lowered below 6.5 MHz. Above the transition point, the velocity distribution of the cloud is isotropic, as shown in Fig. 2(a). Just below the transition point, a narrow peak due to the condensate appears in the center of the distribution, as shown in Figs. 2(c) and 2(d). The narrow peak is elliptical because the condensate retains the asymmetry of the trap. A series of images of this narrow peak shows that its ellipticity reverses in time, with the narrow axis along the TOP trap symmetry axis at early times. This occurs because of the greater repulsive forces associated with the condensate self-energy along the more strongly confining (axial) direction in the trap [7,21]. At lower ν_{final}, the narrow condensate peak becomes more pronounced relative to the broad thermal background, as shown in Figs. 2(e) and 2(f), and at still lower ν_{final} we observe clouds with no obvious thermal pedestal.

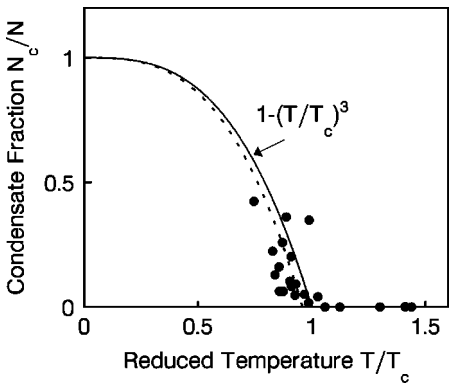

FIG. 3. Condensate fraction N_c/N as a function of the reduced temperature T/T_c, where T_c is the theoretical critical temperature for a noninteracting, trapped Bose gas in the thermodynamic limit. Each data point is an average of several measurements. The solid line is the curve $N_c/N = 1-(T/T_c)^3$. The dashed line shows the best-fit curve $N_c/N = 1-(T/T_c^{expt})^3$, where the best-fit value is $T_c^{expt} = 0.96\pm0.15T_c$.

In order to analyze these data, we fit each image to the sum of a broad symmetric Gaussian and a narrow asymmetric Gaussian. We extract the total atom number N from the integrated total optical density to an accuracy of about 20%; this number agrees with the number estimated from a calibrated laser-induced fluorescence measurement. We also obtain the number of atoms in the condensate N_c from the integrated optical density of the fitted narrow Gaussian. We obtain the temperature T of the atoms from the width of the broad Gaussian to an accuracy of 15%, limited by uncertainties in the magnification of the absorption image, and possible errors resulting from a departure of the fitting function relative to the true cloud shape [23].

The results of the analysis of the data with ν_{final} between 6.8 and 6.25 MHz are shown in Fig. 3. In the figure, we plot the condensate fraction N_c/N, as a function of the reduced temperature T/T_c, where T_c is the theoretical critical temperature for a noninteracting gas in a three-dimensional harmonic trap in the thermodynamic limit, given by [22]

$$kT_c = \hbar\bar{\omega}(N/1.202)^{1/3}, \tag{1}$$

where $\bar{\omega}$ is the geometric mean of harmonic trap frequencies. The BEC transition is reached in the compressed trap at a

temperature near 430 nK, with about 1.5×10^6 atoms in the trap. When the temperature is below T_c, the theoretical condensate fraction is [22]

$$N_c/N = 1-(T/T_c)^3, \tag{2}$$

which we also show in Fig. 3 as a solid line. We find that the data are in good agreement with ideal-gas theory. Fitting the data to Eq. (2), but replacing T_c by a fit parameter T_c^{expt}, we find $T_c^{expt}=(0.96\pm0.15)T_c$. Thus, we do not detect any departure of the transition temperature from ideal-gas theory within our experimental error. Similar results were previously obtained with lower atom number [14]. Larger condensate fractions were obtained with still lower rf stopping frequencies, but we could not obtain an accurate fit for the temperature in that case. With an rf stopping frequency of 6.15 MHz, we found that we could produce a Bose-condensed cloud of as many as 2×10^5 atoms without any obvious thermal tail. We also observed Bose-Einstein condensation of the $F=1$, $m_F=-1$ state of ^{87}Rb, under very similar trapping and evaporation conditions, and with similar numbers of atoms.

In conclusion, we have achieved Bose-Einstein condensation of up to 2×10^5 ^{87}Rb atoms in a TOP trap. This demonstration of relatively large condensates extends the usefulness of the TOP trap as a source of Bose-condensed atoms. Advantages of the TOP trap are that it provides strong confinement and modest asymmetry at the same time, and that it is easy to imagine variations of the TOP that reshape the potential or introduce time dependence into it. Therefore the ability to produce large condensates in a TOP trap should prove useful for a variety of future studies of BEC. Possible directions include further studies of multicomponent Bose condensates [2], precise measurements of condensate thermodynamic and optical properties, condensate excitations including possible nonlinear effects, finite-size effects, and coherence properties.

We are grateful to Eric Cornell, Carl Wieman, Wolfgang Ketterle, Mike Matthews, and Dan Kurn for helpful discussions. We acknowledge the support of National Science Foundation, the R.A. Welch Foundation, and the NASA Microgravity Research Division.

[1] M. H. Anderson, J. R. Ensher, M. R. Matthews, C. E. Wieman, and E. A. Cornell, Science **269**, 198 (1995).
[2] C. J. Myatt, E. A. Burt, R. W. Ghrist, E. A. Cornell, and C. E. Wieman, Phys. Rev. Lett. **78**, 586 (1997).
[3] U. Ernst, A. Marte, F. Schreck, J. Schuster, and G. Rempe, Europhys. Lett. **41**, 1 (1998).
[4] B. Anderson and M. Kasevich (unpublished).
[5] C. C. Bradley, C. A. Sackett, and R. G. Hulet, Phys. Rev. Lett. **78**, 985 (1997).
[6] K. B. Davis, M.-O. Mewes, M. R. Andrews, N. J. van Druten, D. S. Durfee, D. M. Kurn, and W. Ketterle, Phys. Rev. Lett. **75**, 3969 (1995).
[7] M.-O. Mewes, M. R. Andrews, N. J. van Druten, D. M. Kurn, D. S. Durfee, and W. Ketterle, Phys. Rev. Lett. **77**, 416 (1996).
[8] L. V. Hau, B. D. Busch, C. Liu, Z. Dutton, M. M. Burns, and J. A. Golovchenko (unpublished).
[9] M. R. Andrews, C. G. Townsend, H.-J. Miesner, D. S. Durfee, D. M. Kurn, and W. Ketterle, Science **275**, 637 (1997).
[10] W. Ketterle and N. J. Van Druten, Adv. At., Mol., Opt. Phys. **37**, 181 (1996).
[11] W. Petrich, M. H. Anderson, J. R. Ensher, and E. A. Cornell, Phys. Rev. Lett. **74**, 3352 (1995).
[12] K. B. Davis, M.-O. Mewes, M. A. Joffe, M. R. Andrews, and W. Ketterle, Phys. Rev. Lett. **74**, 5202 (1995).
[13] D. S. Jin, J. R. Ensher, M. R. Matthews, C. E. Wieman, and E. A. Cornell, Phys. Rev. Lett. **77**, 420 (1996); D. S. Jin, M. R. Matthews, J. R. Ensher, C. E. Wieman, and E. A. Cornell, *ibid.* **78**, 764 (1997).
[14] J. R. Ensher, D. S. Jin, M. R. Matthews, C. E. Wieman, and E. A. Cornell, Phys. Rev. Lett. **77**, 4984 (1996).
[15] A similar number of Bose-condensed atoms in a TOP trap to ours has also recently been obtained by the JILA group [Eric Cornell (private communication)].
[16] T. E. Barrett, S. W. Dapore-Schwartz, M. D. Ray, and G. P. Lafyatis, Phys. Rev. Lett. **67**, 3483 (1991).
[17] E. L. Raab, M. Prentiss, A. Cable, S. Chu, and D. Pritchard, Phys. Rev. Lett. **59**, 2631 (1987).
[18] W. Ketterle, K. B. Davis, M. A. Joffe, A. Martin, and D. E. Pritchard, Phys. Rev. Lett. **70**, 2253 (1993).
[19] C. G. Townsend, N. H. Edwards, K. P. Zetie, C. J. Cooper, J. Rink, and C. J. Foot, Phys. Rev. A **53**, 1702 (1996).
[20] H. M. J. M. Boesten, C. C. Tsai, J. R. Gardner, D. J. Heinzen, and B. J. Verhaar, Phys. Rev. A **55**, 636 (1997).
[21] Y. Castin and R. Dum, Phys. Rev. Lett. **77**, 5315 (1996); M. J. Holland, D. S. Jin, M. L. Chiofalo, and J. Cooper, *ibid.* **78**, 3801 (1997).
[22] V. Bagnato, D. E. Pritchard, and D. Kleppner, Phys. Rev. A **35**, 4354 (1987).
[23] R. J. Dodd, K. Burnett, M. Edwards, and C. W. Clark, cond-mat/9721186.